



Article

Parametric Optimization of Isotropic and Composite Axially Symmetric Shells Subjected to External Pressure and Twisting

Marek Barski *, Paweł J. Romanowicz , Małgorzata Chwał and Adam Stawiarski

Chair of Machine Design and Composite Structures, Cracow University of Technology, Ul. Warszawska 24, 31-155 Krakow, Poland; pawel.romanowicz@pk.edu.pl (P.J.R.); malgorzata.chwal@pk.edu.pl (M.C.); adam.stawiarski@pk.edu.pl (A.S.)

* Correspondence: marek.barski@pk.edu.pl

Abstract: The present paper is devoted to the problem of the optimal design of thin-walled composite axially symmetric shells with respect to buckling resistance. The optimization problem is formulated with the following constraints: namely, all analyzed shells have identical capacity and volume of material. The optimization procedure consists of four steps. In the first step, the initial calculations are made for cylindrical shells with non-optimal orientation of layers and these results are used as the reference for optimization. Next, the optimal orientations of layers for cylindrical shapes are determined. In the third step, the optimal geometrical shape of a middle surface with a constant thickness is determined for isotropic material. Finally, for the assumed shape of the middle surface, the optimal fiber orientation angle θ of the composite shell is appointed. Such studies were carried for three cases: pure external pressure, pure twisting, and combined external pressure with twisting. In the case of shells made of isotropic material the obtained results are compared with the optimal structure of uniform stability, where the analytical Shirshov's local stability condition is utilized. In the case of structures made of composite materials, the computations are carried out for two different materials, where the ratio of E_1/E_2 is equal to 17.573 and 3.415. The obtained benefit from optimization, measured as the ratio of critical load multiplier computed for reference shell and optimal structure, is significant. Finally, the optimal geometrical shapes and orientations of the layers for the assumed loadings is proposed.

Keywords: axially symmetric shells; buckling; parametric optimization; external pressure; twisting; composite materials



Citation: Barski, M.; Romanowicz, P.J.; Chwał, M.; Stawiarski, A. Parametric Optimization of Isotropic and Composite Axially Symmetric Shells Subjected to External Pressure and Twisting. *J. Compos. Sci.* **2021**, *5*, 128. <https://doi.org/10.3390/jcs5050128>

Academic Editor: Francesco Tornabene

Received: 17 April 2021
Accepted: 7 May 2021
Published: 12 May 2021

Publisher's Note: MDPI stays neutral with regard to jurisdictional claims in published maps and institutional affiliations.



Copyright: © 2021 by the authors. Licensee MDPI, Basel, Switzerland. This article is an open access article distributed under the terms and conditions of the Creative Commons Attribution (CC BY) license (<https://creativecommons.org/licenses/by/4.0/>).

1. Introduction

Axially-symmetric, thin-walled structures have received considerable attention mainly due to their practical applications such as underwater pressure hulls, space vehicles, or pressure tanks [1–4]. Material and structural optimization becomes a central concept in their design because of the adaptability of composite materials to given design situations/requirements. To achieve an optimized structure with improved characteristics (buckling resistance), not only design parameters such as layer thicknesses and ply angles (stacking sequence configuration) can be employed but also shape/topology of thin-walled shells should be taken into account.

In general, the shape/topology optimization methods for improving buckling capacity are based on the variations of the shell meridian (with a positive Gaussian curvature) that can be represented in the form of ellipsoids, barrel-shaped, egg-shaped, or Cassini curves [2–13]. Unfortunately, the thin-walled structures are highly sensitive to the buckling phenomena. Moreover, the geometrical shape of the middle surface, variable or constant wall thickness, material properties as well as different forms of imperfections have a significant impact on this problem [9–15].

Among different axially-symmetric shapes of the shells, the so-called barrel-shaped structures are of special interest. Parametric optimization due to loss of stability of barrel-

shaped shells subjected to axial compression and a combination of axial compression and pressure was presented by Błachut [16,17]. The experimental and numerical results of buckling of barrel-shaped shells under external pressure were reported by Błachut [18]. A good agreement between them was observed. The numerical simulations were carried out with the use of Abaqus. In the case of barrel-shaped shells, the critical pressure could be significantly higher in comparison with cylindrical shells with an equivalent volume of material. Finally, the optimal shape of the middle surface was determined by Błachut [19] with the use of the simulated annealing algorithm. The shape of the middle surface was described by the super-ellipse, where the parameters of this curve were considered as design variables.

The buckling phenomenon of the barrel-shaped shells was also studied by Jasion and Magnucki [20]. They analyzed the impact of a decreasing radius of meridional curvature on the value of critical external pressure. Next, Jasion [21] investigated the axially-symmetric shells with positive and negative Gaussian curvature under external pressure. Two kinds of analysis with the use of ABAQUS software were conducted, namely linear eigenvalue buckling prediction and fully non-linear post-buckling analysis. A significant difference in the behavior of the shells with negative Gaussian curvature and barrel-shaped shells was observed. In the post-buckling range, the latter shells reveal the unstable load-deflection path. Jasion and Magnucki [22] also studied the buckling phenomenon of barrel-shaped tanks filled with liquid. Finally, Magnucki and Jasion [23] investigated the buckling of the barrel-shaped shell subjected to radial pressure. The problem was described analytically and solved approximately with the use of Bubnov's-Galerkin's method. Next, the analytical results were verified with the use of the finite element method. A good agreement of the analytical and numerical results (membrane stresses, buckling load, and buckling shape) was reported.

Here it is worth noting that the external load can be also defined as the displacement of the particular part of a thin-walled structure. The example of this kind of buckling problem was presented and discussed on the example of the thin-walled column by Stawiarski and Kruzelecki [24].

Very interesting works, which concern the buckling phenomena of the egg-shaped shells subjected to external pressure, were presented by Zhang and his colleagues [25–27]. In the first work, the influence of the geometrical dimensions on the critical buckling load was investigated. The shape of the middle surface mimics that of the goose egg. The analysis was carried out numerically in ABAQUS and compared with the analytical solution. Next, the non-linear buckling analysis was performed for the variable and constant thickness shells. The obtained results were also verified experimentally. Finally, the impact of the geometrical imperfection on the buckling and post-buckling behavior was also investigated.

The barrel-shaped, pseudo-barrel, and cylindrical shells of a constant mass with the corrugated middle surface were analyzed by Sowiński [28]. The problem of elastic stability of these structures was solved with the use of the finite element method. The explicit finite element solvers (LS-DYNA) were also used for the dynamic buckling behavior of spherical shell structures colliding with an obstacle block under the sea [4]. There were also proposed finite elements for nonlinear buckling and post-buckling analyses of plates and shells subjected to large deflection and rotation [29,30].

Życzkowski and Kruzelecki [31] determined the optimal shape of a cylindrical shell loaded by overall bending moment with the use of the stability constraint in the local form. Moreover, they proposed a concept of the shell of uniform stability. This concept was next utilized by Kruzelecki and Trzeciak [32] in the case of optimal design of axially-symmetric shells under hydrostatic pressure and by Życzkowski et al. [33] for buckling of axially-symmetric shells under thermal load. In order to obtain the solution of the optimization problem the variational approach was applied. Barski and Kruzelecki [34–36] and Barski [37] used the simulated annealing algorithm and Bezier's curves in order to obtain the solution of the optimization problem of shells subjected to combined loadings.

Such studies were carried for the following loading conditions: bending moment with shearing force taken into account, bending moment, axial force and twisting, and finally bending moment and external hydrostatic pressure. The concept of the shell of uniform stability was also utilized. The relationship, which describes the distribution of the wall thickness is not available in the analytical closed form. Therefore, the special, iterative algorithm for wall thickness estimation was also developed. In the latter work, the shape of the transversal cross-section of the middle surface was also optimized.

The experimental and theoretical studies of buckling and post-buckling behavior of composite shell structures were recently discussed and presented in the papers [38–44]. Such analyses were related to the structures with cut-outs and reinforcements [38], local damages [39], multilayered composite shells [40], honeycomb cylindrical shells [41], conical shells [42], and local buckling of multilayered shells and plates with cut-out under tensile loadings [43,44]. Concluding the above-mentioned studies, it can be said that an advantage of using fiber-reinforced composites over conventional metallic materials is that the former can be tailored to specific requirements of certain applications. However, the large number of design variables (i.e., fiber orientations angles and thicknesses of a particular layer) and the complex mechanical behavior associated with such materials make the structural design much more complex than those involving conventional materials. Also, for many 2D design problems (beams, plates, and shells), there are multiple designs with similar performance. These designs may have very different stacking sequences, but very similar or almost identical values of the extensional [A], coupling [B], and bending [D] stiffness matrices. Moreover, the number of design variables is strongly affected by the type of kinematical hypothesis used. Broad reviews of the existing approaches to the definition of design variables were presented by Verchery [45] and Muc and Chwał [46]. In such cases, it is important to produce all or most design alternatives. It is necessary to point out that the effectiveness of the optimum design, especially for composite structures, strongly depends on the proper choice of two elements: (i) the type of design variables and (ii) an appropriate optimization algorithm.

Generally, the discussed above papers mainly concern the barrel-shaped shells made of isotropic material. However, in the case of composite structures, the shape of the middle surface and the optimal configuration of the composite material (orientation of the layers) should be optimized. Therefore, such an optimization problem seems to be very difficult to solve. The main novelty of the currently presented approach is that the optimization problem is split into two steps. In the first step, the optimal shape of the middle surface is looked for. Next, for the optimal shape of the middle surface, the optimal configuration of the material is estimated. Both steps are realized by relatively simple procedures. However, the proposed approach seems to be very fast, robust, effective, and leads to a reliable solution. According to the author's knowledge, the works where these two optimization problems (shape of the middle surface and configuration of the composite material) are studied at the same time are very rare. The current work is devoted to the problem of optimal design of the composite thin-walled and barrel-shaped structures. The shape of the middle surface, as well as the configuration of composite material are optimized, for which the external load reaches the maximum concerning elastic static buckling.

The paper consists of five sections and two appendices (Appendices A and B). The introduction and literature review are presented in Section 1. The formulation of the investigated problem as well as a description of the design variables is given in Section 2. The description of the numerical model and the method of optimization is discussed in Section 3. The results of the performed studies, including optimization of the axially symmetric shells to three different loading conditions (pure external pressure, pure twisting, complex twisting with external pressure) for three different isotropic and composite materials are presented and discussed in Section 4. The most important results and conclusions are summarized in Section 5. Moreover, some necessary formulations are given in Appendix A. The analytical model applied in the optimization technique and its verification with the use of the finite element analyses is also presented in detail in Appendix B.

2. Formulation of Optimization Problem

The subject of the optimization is the axially symmetric barrel-shaped shell presented in Figure 1. The total length of the analyzed structure is designated as L_0 and constant uniform thickness as H . It is assumed that the structure is subjected to three different loading conditions: pure external hydrostatic pressure p_0 , pure twisting moment M_t , and a combined load, which consists of external hydrostatic pressure p_0 and twisting moment M_t .

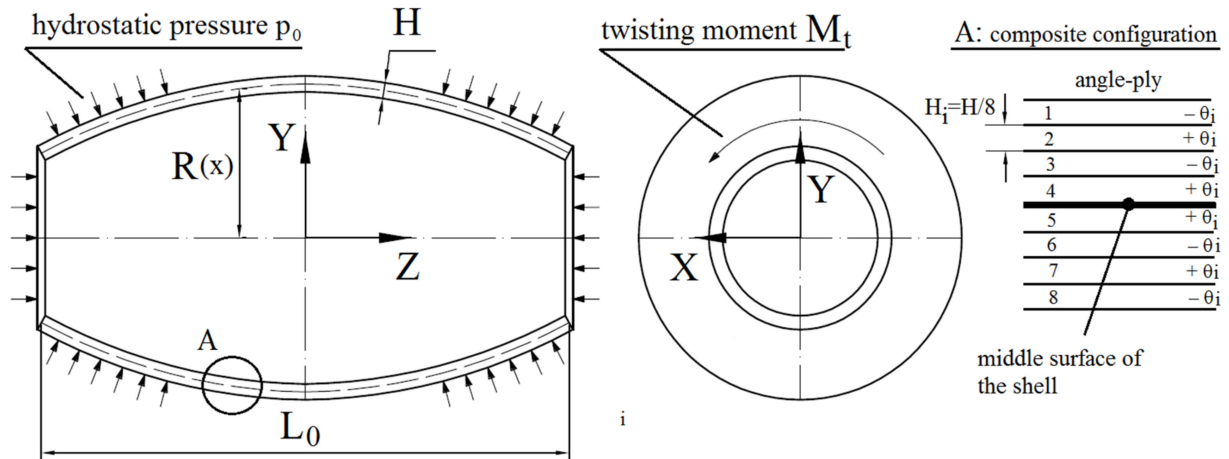


Figure 1. Investigated shell under combined loadings.

Each layer of a laminate can be identified by its location in the laminate (the pair $z_i, z_{i-1}, i = 1, \dots, N$ —the total number of plies), its fiber orientation θ_i (Figure 1), and material properties. Let us assume that each ply in the laminate is made from the same composite material. The value of the external pressure p_0 is defined as the load multiplier. The twisting moment M_t , which acts at both ends of the structure is expressed as follows:

$$M_t = m_t \pi p_0 R_0^3 \tag{1}$$

where: m_t is the dimensionless parameter introduced to have a possibility for free choice of the magnitude of the twisting moment ($m_t = 0$ means that the twisting moment does not act), and R_0 denotes a constant radius of cylindrical reference shell of a constant length L_0 and a constant thickness H_0 . Due to the fact that the studied structure is loaded by uniformly distributed hydrostatic pressure p_0 , which acts on the end caps as well, the axial compression has to be taken into account (see Appendix B, Equation (A16)). To eliminate a ‘circumferential bending’ of the wall of a shell under hydrostatic pressure and take advantage of membrane stresses under this load, our considerations are limited to shells with the axially symmetric shape of a middle surface. In other words, a circular profile of the cross-section constitutes a necessary condition of a membrane state for shells under uniform pressure (Vlassov [47]).

The geometry of the investigated shell is uniquely defined when the shape of a middle surface, as well as wall thickness, is determined. As is mentioned above, our considerations are restricted to the axially symmetric shape of a middle surface, where the profile of each cross-section of a shell is a circle. Thus, the radius of longitudinal R_1 and circumferential R_2 curvature are given as follows:

$$R_1 = \frac{(1 + R'^2)^{\frac{3}{2}}}{-R''}, R_2 = R(1 + R'^2)^{\frac{1}{2}} \tag{2}$$

where $(\prime) = d/dx$ and R is a distance from the axis of a structure to a point of a middle surface. Moreover, it is assumed that the wall thickness H of a studied structure is constant (it is not a design variable) and its value is to be determined from the optimization constraint,

which presumes that the optimal structure and reference shell have the same volume of material. Due to the symmetry of the structure, only the right-hand part of a shell, namely $0 \leq x \leq L_0/2$, is to be only considered, and the condition $R'(0) = 0$ of symmetry of the structure is assumed.

Finally, it is assumed that the investigated structure is made of an isotropic material (where the mechanical properties are described by Young’s modulus E_0 and Poisson’s ratio ν_0) as well as transversely isotropic composite material (where the mechanical properties are described at last by $E_1, E_2, G_{12}, \nu_{12}$) of symmetric, angle-ply configuration. Such a configuration is uniquely defined by a single quantity, namely the value of fiber orientation angle $\pm\theta^\circ$. The applied symmetric composite material consists of eight layers of equal thickness, where $H_i = H/8, i = 1, 2, \dots, 8$ with layers orientations defined as $[-\theta, +\theta, -\theta, +\theta]_S$.

Thus, the optimization problem can be stated as follows. We look for such a structure, for which the value of the critical loading parameter $p_0 = p_{cr}$ reaches the maximum, namely:

$$p_{cr} \Rightarrow \max \tag{3}$$

Design variables are considered with the following quantities: (a) shape of the middle surface, which is described by function $R = R(x)$ and (b) the fiber orientation angle $\pm\theta^\circ$ in the composite material of angle-ply configuration. It is assumed that the shape of the middle surface is described by a simple parametric formula, namely:

$$R(x) = R^c \left(1 - m \left(\frac{2 \cdot x}{L_0} \right)^2 \right) \tag{4}$$

The parameter R^c denotes the radius of the middle surface measured in the geometrical center of the shell, $R^c = R(0)$, the value of which will be determined later. In the performed study, the parameter m is assumed as the design variable, which defines the geometrical shape of the middle surface of the shell. In other words, parameters m and θ are considered as the design variables. The optimization problem is defined as stated above under the following constraints:

1. The volume of the material of the optimal structure and reference shell is identical.
2. The capacity of the optimal structure and reference shell is equal.
3. The minimal radius at both ends of the shell is constrained by a lower bound, $R(L_0) > R_{adm}$.
4. The slope of the meridian is limited by upper bound, $|R'| \leq R_{adm}$.
5. The current study is limited to the convex shell (the positive Gaussian curvature), where $R'' \leq 0$.

The lower bound values are assumed as follows $R_{adm} \geq 0$ and $R'_{adm} \geq 0$. The value of parameter R^c in definition (4) for the assumed value of m is determined with the use of equality constraint (2) (constraint (A2) in Appendix A). Further, it should be noted here that the value of the wall thickness of the optimal structure can be readily computed with the use of the equality constraint (1) (constraint (A1) in Appendix A) from the list presented above. Moreover, there is no defined restriction imposed on the wall thickness, for example, lower or upper bound. Restrictions can lead to non-smooth structures, which are not allowed in the present study. All necessary formulas, as well as dimensionless definitions of the particular quantities, are discussed in Appendix A.

3. Methods of Finding Solution

3.1. Optimization Procedure

The method proposed here of description of the shape of the middle surface by Equation (4) seems to be very simple. However, according to the author’s experience [34–37], the differences between the results obtained from proposed here with a parametric optimization procedure and the results obtained with the use of analytical methods (variational

approach) or other advanced numerical algorithms, where the shape of the middle surface is described by, for example, Bézier's curves, are not significant and does not exceed 7%. On the other hand, the simple parametric procedure is very effective and always provides a good estimation of the global optimum. Moreover, in the case of advanced optimization algorithms, like evolutionary algorithms or simulated annealing algorithms, the number of calls of objective function significantly increases in comparison with the parametric procedure.

Although the current paper concerns mainly the shell of the uniform thickness, the obtained results of optimization can be readily compared with the results, which one can get when the shell of uniform stability is assumed. The condition "the shell of uniform stability" means that local stability is satisfied in the form of equality not only at a dangerous point but at any point of a shell. In the latter case, the solution of the optimization problem can be found easily with the use of simple analytical formulas, which are detailed discussed in Appendix B. Moreover, this comparison can be done in two possible cases. In the first case, having previously determined the optimal shape of the middle surface, the distribution of the wall thickness is computed with the use of the Shirshov's local buckling condition (Appendix B) [48]. In the second case, the optimal shape of the middle surface is looked for together with the optimal distribution of the wall thickness. Thus, the optimal shape of the middle surface can be slightly different in comparison with the shape, which is obtained when the shell of uniform thickness is assumed. It is rather obvious that the highest profit from optimization should be expected in the last case. It is worth noting here that Shirshov's local stability condition has an approximate character. Therefore, a special procedure, which is based on the finite element method, designed to verify the accuracy and effectiveness of the Shirshov's local stability condition and other necessary analytical formulas describing mainly the membrane resultant stresses, is also described in Appendix B.

In the second step of the optimization procedure, for the previously found optimal shape of the middle surface, the optimal fiber orientation angle θ is looked for. It is assumed that now the studied structure is made of the composite material which is symmetric to the middle surface, angle-ply configuration. As is mentioned above, the applied composite material consists of 8, equally thick $H_i = H/8$, $i = 1, 2, \dots, 8$ layers. It is assumed that the feasible fiber orientation angles θ belong to the range $[0^\circ, 90^\circ]$. The solution of the optimization problem is estimated by repeatedly computing the critical buckling load multiplier q_{cr} for the starting value of the angle θ equal to 0° and increment $d\theta = 5^\circ$. From among the 19 calculated values of the critical load multiplier q_{cr} , as a solution of the optimization problem, a value of the angle θ is to be chosen, for which the value of critical load multiplier q_{cr} is the highest. It is worth noting here that for smaller angle increment $d\theta$, the obtained solutions do not vary significantly. The fiber orientation angle is assumed to be $\theta = 0^\circ$ when the fiber is parallel to the circumferential direction.

3.2. Numerical Model and Material Properties

In order to compute the critical buckling load multiplier q_{cr} the finite element method is applied. The whole calculations are carried out with the use of commercially available software ANSYS 13.0. The investigated structure is modeled as a shell with the use of higher-order SHELL281 elements. These elements have in each node three translational and three rotational degrees of freedom. As is shown in Figure 2, the regular mapped mesh is applied. Assuming a cylindrical global coordinate system, where the axis of symmetry is Z-axis (Figure 1), the imposed boundary conditions are as follows: for $Z = -L_0/2$, and $Z = L_0/2$, $U_R = 0$ and for $Z = 0$, $U_Z = 0$ (symmetry condition), where U_R and U_Z is the radial and axial component of displacement, respectively. Moreover, to eliminate the possibility of rigid rotation about axis Z of the whole structure, for $Z = 0$, $U_\theta = 0$, which is prescribed in any single point, where U_θ is the circumferential component of displacement. The external hydrostatic pressure is modeled as a normal surface load applied to all elements. The axial

compression, caused by external pressure, as well as twisting, is applied to both ends of the shell as a nodal force FZ and $F\theta$, the values of which are:

$$FZ = \pm \frac{\pi R(\pm 0.5L_0)^2 p_0}{N}, F\theta = \pm \frac{m_t \pi R_0^2 p_0}{N} \tag{5}$$

where N is a total number of nodes, which are located at the end edges of the structure. The ‘ \pm ’ sign denotes that the returns of the $F\theta$ at the ends of the shell have to be the opposite. The obtained values of critical buckling load multiplier in the case of external pressure and twisting for simple cylindrical shells made of isotropic material agrees with those (theoretical and empirical) which are presented by Bushnell [49].

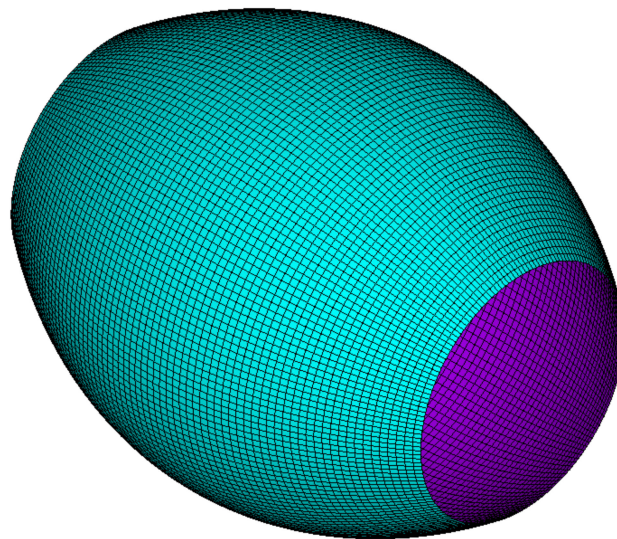


Figure 2. Finite element model of investigated shell for $\mu = 0.375$, $R(\xi = 0) = 1.153$, $m = 0.425$.

The calculations are performed for the shell of constant total length $L_0 = 1000$ mm, and of the following radius $R_0 = 500, 375, 250, 187.5, 125$ mm. Taking into consideration the dimensionless quantities, which are presented in Appendix A (Equation (A3)), it corresponds to $\mu = R_0/L_0 = 0.5, 0.375, 0.25, 0.188, 0.125$. Moreover, the computations are carried out for two values of a parameter $\gamma = H_0/R_0 = 0.004, 0.008$. Therefore, in the first case $H = 2, 1.5, 1, 0.75, 0.5$ mm and in the second case $H = 4, 3, 2, 1.5, 1$ mm. Finally, after performing the appropriate convergent tests of numerical solutions, it is assumed that the size of the finite element is equal to $l_e = 15$ mm in all cases.

In the first step of the optimization procedure, the applied isotropic material is assumed to be steel. In the second step of the optimization problem, there are considered to be two different composite materials, namely carbon fibers/epoxy resin and glass fibers/polyester resin. The mechanical properties of the applied materials are collected in Table 1.

Table 1. Mechanical properties of applied materials [50,51].

Material	E_1 [GPa]	E_2 [GPa]	G_{12} [GPa]	ν_{12}	E_1/E_2
steel	210.0	210.0	80.77	0.30	1.000
carbon fiber/epoxy resin	181.0	10.3	7.17	0.28	17.573
glass fiber/polyester resin	28.0	8.2	2.80	0.29	3.415

4. Results

The computations are carried out separately for the shells subjected to pure hydrostatic pressure (Section 4.1), pure twisting (Section 4.2), and finally for different combinations of mentioned previously components of loading (Section 4.3). The optimization procedure is

applied to the above three loading cases, in which different materials and geometries were investigated. According to the optimization procedure, which is described in Section 3, the results are presented in two parts.

The first part for each particular loading condition is related to the optimization of the geometry of the isotropic barrel shell. This optimal barrel shape shell curvature is described by the determined radii $r(0)$ and $r(1)$ or parameter m . For such purpose, the dimensionless values of the critical buckling load multiplier computed for the reference q_0 , for the optimal shell q^{max} , and for the shell of uniform stability q^{ustb} are calculated using the Formula (A3). It is assumed that associated shells of uniform stability have the same shape of the middle surface as the structures, which are the solution of the optimization problem. The values q^{ustb} are computed according to the analytical formulas discussed in Appendix B. Finally, n and n_0 refer to the number of the circumferential half-waves measured in the circumferential direction for the optimal and reference shell, respectively.

In the second part of each optimization procedure, there are performed calculations for transversely anisotropic cylindrical and barrel shells. First of all, the calculations are made for cylindrical geometry with orientations of fibers $\theta = 90^\circ$. This allows for the determination of the value of the critical load multiplier for reference structure designated as q^{com}_0 . In the next step, the optimal fiber orientation angle for cylindrical shell θ_{cyl} is determined. It should be noted, that the layers orientations are defined as $[-\theta_{cyl}, +\theta_{cyl}, -\theta_{cyl}, +\theta_{cyl}]_S$, as is presented in Figure 1. For the optimal configuration of the layers in the cylindrical shell, the maximum load multiplier for cylindrical shell q^{com}_{cyl} is calculated. The results are presented in the form of the ratio q^{com}_{cyl} and q^{com}_0 , which gives information concerning the increase of the critical buckling load in the optimal cylindrical shell. In the final step, the optimal configuration of the fibers orientation angle θ^{max} is determined for the optimal barrel shape of the middle surface. The same as for cylindrical shape, it means that the layers orientations for barrel shape shell are defined as $[-\theta^{max}, +\theta^{max}, -\theta^{max}, +\theta^{max}]_S$, as presented in Figure 1.

4.1. Composite Shell under Hydrostatic Pressure

The results of optimization in the case of the shell under hydrostatic pressure are collected in Tables 2–4 and Figures 3 and 4. The determined optimal barrel shape geometries for the isotropic shell are summarized in Table 2. Generally, the optimal shape of the middle surface is far from the cylinder. It is worth noting here that starting from $\mu = 0.25$ the inequality constraint (3), which limits the length of the radius of the shell at both ends is active, $r(1) \geq 0.5$. The highest profit from optimization is observed for the shells for which the parameter μ is relatively large. Together with decreasing the value of ratio μ , the profit from optimization also decreases. However, in the case of $\mu = 0.25$, the profit is slightly higher in comparison with the shell, where $\mu = 0.375$. It can be explained by the fact, that for that structure ($\mu = 0.25$) the character of the observed buckling pattern is changed, which is shown in Table 5.

Table 2. Results of optimization for shell under hydrostatic pressure.

μ	$q_0 \cdot 10^{-6}$	q^{max}/q_0	q^{ustb}/q_0	h	n/n_0	$r(0)$	$r(1)$
$\gamma = 0.004$							
0.500	2.500	3.461	3.767	0.937	36/16	1.115	0.753
0.375	2.162	3.476	3.693	0.938	32/14	1.159	0.647
0.250	1.773	3.570	3.547	0.961	28/10	1.216	0.500
0.188	1.517	3.220	3.233	0.987	30/10	1.216	0.500
0.125	1.223	2.670	2.750	1.007	20/8	1.216	0.500
$\gamma = 0.008$							
0.500	11.811	3.012	3.189	0.937	26/12	1.115	0.753
0.375	10.364	2.980	3.082	0.938	24/12	1.159	0.647
0.250	8.457	3.046	2.975	0.961	22/10	1.216	0.500
0.188	7.115	2.761	2.757	0.987	22/8	1.216	0.500
0.125	5.903	2.238	2.279	1.007	14/6	1.216	0.500

Table 3. Results of optimization for composite shell under external pressure, $E_1/E_2 = 17.573$.

μ	γ	Cylindrical Pipe			Optimal (Barrel) Shape		
		$q^{com}_0 \cdot 10^{-6}$	q^{com}_{cyl}/q^{com}_0	$\theta^{cyl} [^\circ]^1$	q^{max}/q^{com}_0	$\theta^{max} [^\circ]^1$	n/n_0
0.500	0.004	0.781	2.091	10	5.495	15	22/20
0.375		0.683	2.084	0	5.457	10	18/18
0.250		0.569	2.028	0	5.460	0	16/16
0.188		0.495	2.099	5	4.785	0	16/14
0.125		0.411	1.996	0	3.903	0	10/12
0.500	0.008	3.659	2.126	5	4.851	25	18/16
0.375		3.217	2.045	0	4.768	15	14/14
0.250		2.655	2.065	5	4.723	0	12/12
0.188		2.353	1.998	0	4.068	0	10/12
0.125		1.938	2.189	10	3.386	0	8/10

¹ layer orientations are defined as $[-\theta, +\theta, -\theta, +\theta]_S$.

Table 4. Results of optimization for composite shell under external pressure, $E_1/E_2 = 3.415$.

μ	γ	Cylindrical Pipe			Optimal (Barrel) Shape		
		$q^{com}_0 \cdot 10^{-6}$	q^{com}_{cyl}/q^{com}_0	$\theta^{cyl} [^\circ]^1$	q^{max}/q^{com}_0	$\theta^{max} [^\circ]^1$	n/n_0
0.500	0.004	1.489	1.368	0	4.080	10	28/18
0.375		1.300	1.357	0	4.140	0	24/16
0.250		1.053	1.377	0	4.354	0	22/12
0.188		0.913	1.357	0	3.880	0	22/10
0.125		0.741	1.423	0	3.210	0	16/10
0.500	0.008	6.949	1.372	0	3.579	15	22/14
0.375		6.079	1.364	0	3.609	5	18/12
0.250		5.001	1.348	0	3.719	0	16/10
0.188		4.391	1.410	0	3.238	0	16/10
0.125		3.552	1.345	0	2.727	0	12/8

¹ layer orientations are defined as $[-\theta, +\theta, -\theta, +\theta]_S$.

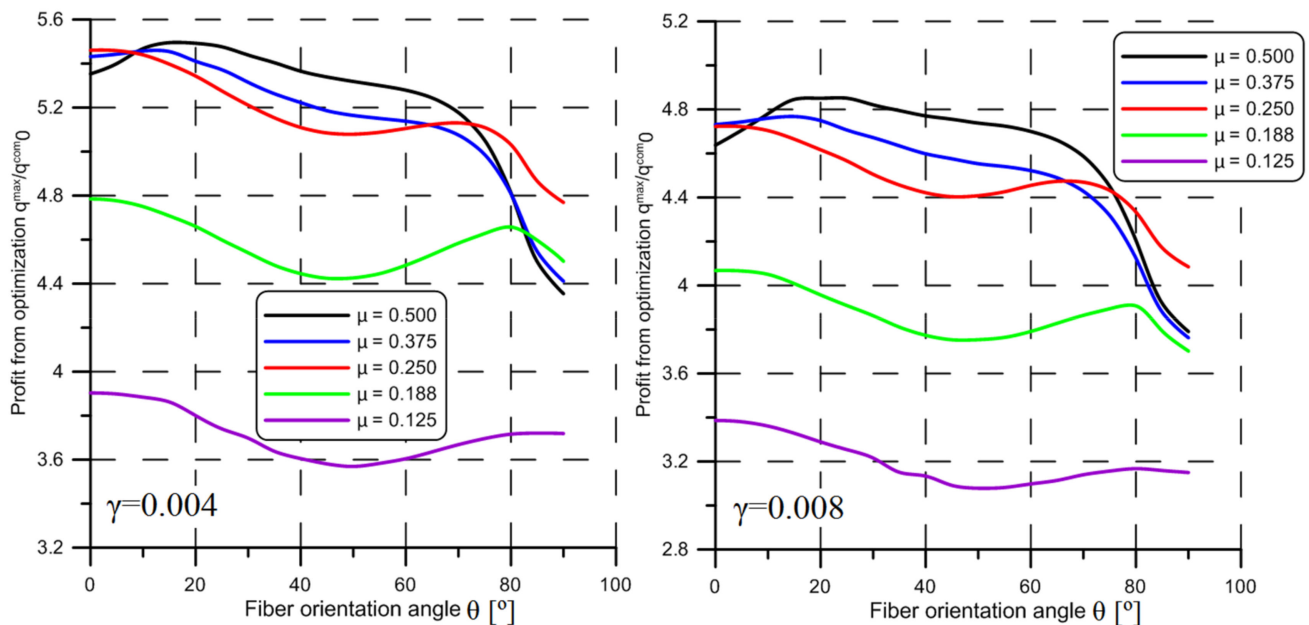


Figure 3. Optimization profit q^{max}/q^{com}_0 as a function of fiber orientation angle θ , $E_1/E_2 = 17.573$.

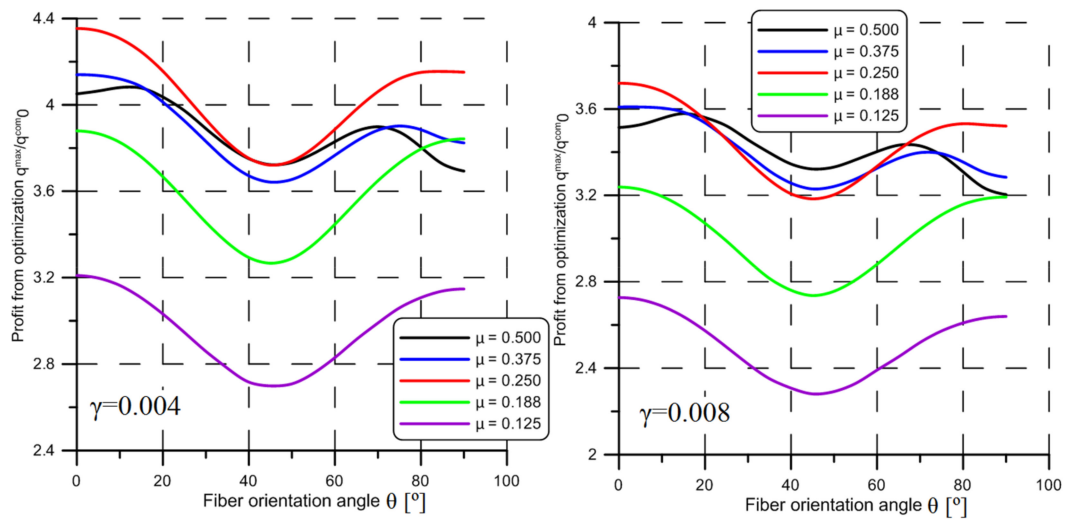
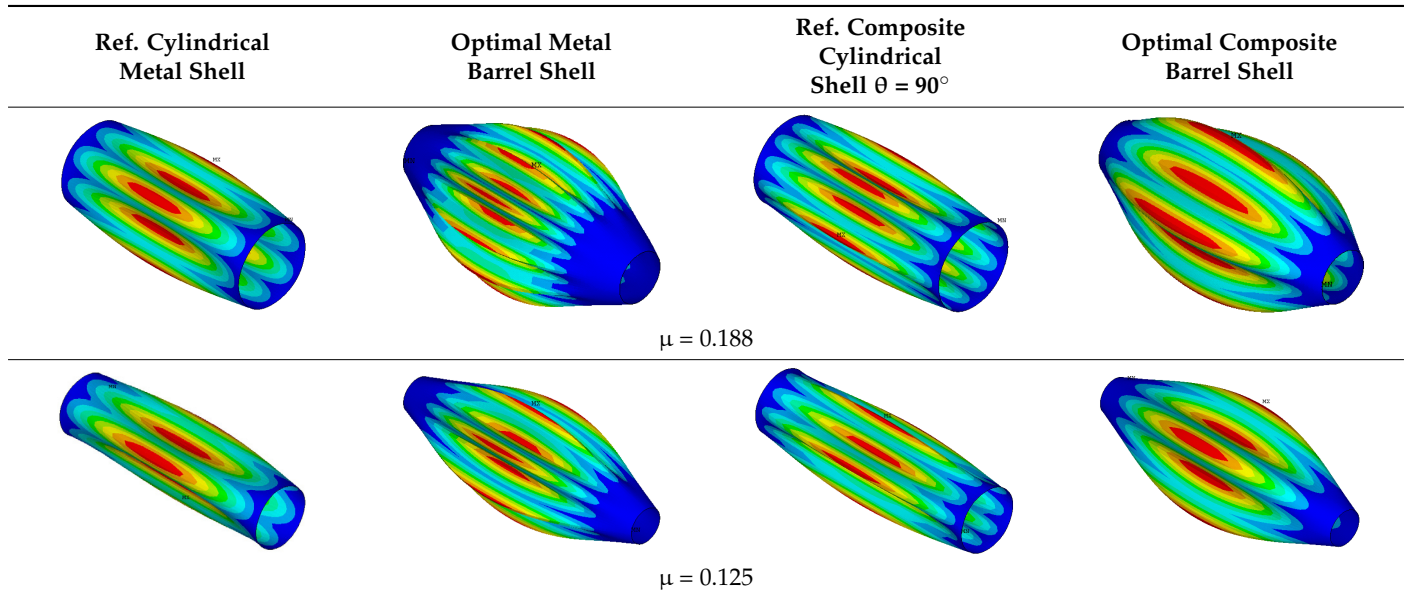


Figure 4. Optimization profit q^{max}/q^{com}_0 as a function of fiber orientation angle θ , $E_1/E_2 = 3.415$.

Table 5. Buckling patterns of reference and optimal shells under external pressure, $\gamma = 0.008$.

Ref. Cylindrical Metal Shell	Optimal Metal Barrel Shell	Ref. Composite Cylindrical Shell $\theta = 90^\circ$	Optimal Composite Barrel Shell
$\mu = 0.500$			
$\mu = 0.375$			
$\mu = 0.250$			

Table 5. Cont.



In Table 5, the corresponding buckling patterns of the cylindrical references are also presented. For shorter shells, the half-waves are observed near both ends. For the longer structures, the buckling pattern is shifted to the center of the structure. Generally, the total number of half-waves for the optimal structure is over two times higher in comparison with the reference one. The obtained profit is also slightly higher for the thinner shells. It is worth stressing here that in the case of the shells of uniform thickness the observed values of h are not very far from the unity. Thus, the thicknesses of the real optimal structures do not vary significantly. Additionally, it should be stressed here that the profit from optimization q^{ustb} , computed under the assumption of the shell of uniform stability, is similar to that which is obtained for the shell of uniform thickness. This is an important conclusion from a practical point of view because the structure of uniform thickness is easier to manufacture.

In the next step of the proposed optimization procedure, the reference structure is changed. Now the reference shell is a cylindrical shell with such an angle-ply configuration for which the critical buckling load multiplier q^{com}_0 reaches the lowest possible value. It occurred that the lowest value of q^{com}_0 is always obtained for fiber orientation angle $\theta = 90^\circ$.

It should be noted here that the curves presented in Figures 3 and 4 are prepared under the assumption that the optimal fiber orientation angle θ is observed for the shell, where the shape of the middle surface is determined previously in the first step of the optimization procedure for isotropic material.

Generally, the profit from optimization increases together with increasing ratio E_1/E_2 . For $E_1/E_2 = 17.573$, the highest values of q^{max}/q^{com}_0 ratio are observed for relatively short structures with parameters $\mu = 0.5$, and $\mu = 0.375$. However, in the case of $E_1/E_2 = 3.415$, the highest value of q^{max}/q^{com}_0 ratio is obtained for the shell with parameter $\mu = 0.25$. For these shells, the optimal fiber orientation angles θ^{max} vary from 5° to 25° . In the case of longer structures $\mu < 0.375$ the optimal angle $\theta^{max} = 0^\circ$. In both cases of E_1/E_2 ratio, the profit from optimization is higher for the shells with parameter $\gamma = 0.004$. In comparison with the cylindrical shells (Tables 3 and 4), the profit from optimization is over two times higher. Thus, one can say that the change of the shape of the middle surface has a decisive impact on the final results. The obtained buckling patterns of optimal structures are very similar to those which are presented in Table 4. Finally, it is worth stressing here that the obtained results, namely the values of q^{max}/q^{com}_0 ratio, are significantly higher in comparison with the results which are presented for isotropic shells for all studied cases.

4.2. Composite Shell under Twisting

The results of optimization of the shell subjected to twisting are presented in Figures 5 and 6 and Tables 6–9. In the case of the shell of uniform thickness, the profit from optimization does not vary significantly with respect to parameter μ as well as γ and it does not exceed $q^{max}/q_0 = 1.712$ (Table 6). In comparison with a shell under external pressure, the profit from optimization is much smaller. Moreover, to the contrary of the shell of uniform stability, together with decreasing parameter μ the profit from optimization slightly increases. A clear discrepancy between the shell of uniform thickness and the shell of uniform stability is observed. The results obtained for the shell of uniform stability are generally worse in comparison with the shell of uniform thickness. As is discussed in Appendix B, these discrepancies can be caused by a very rough estimation of membrane resultant stress caused by twisting. The wall thickness h , like previously in the case of the structure under external pressure, is also very close to unity. This fact is also very important from a practical point of view. For the shells, where μ ratio is equal to $\mu = 0.125$ the wall thickness for the optimal structure is even slightly greater in comparison with the cylindrical reference shell.

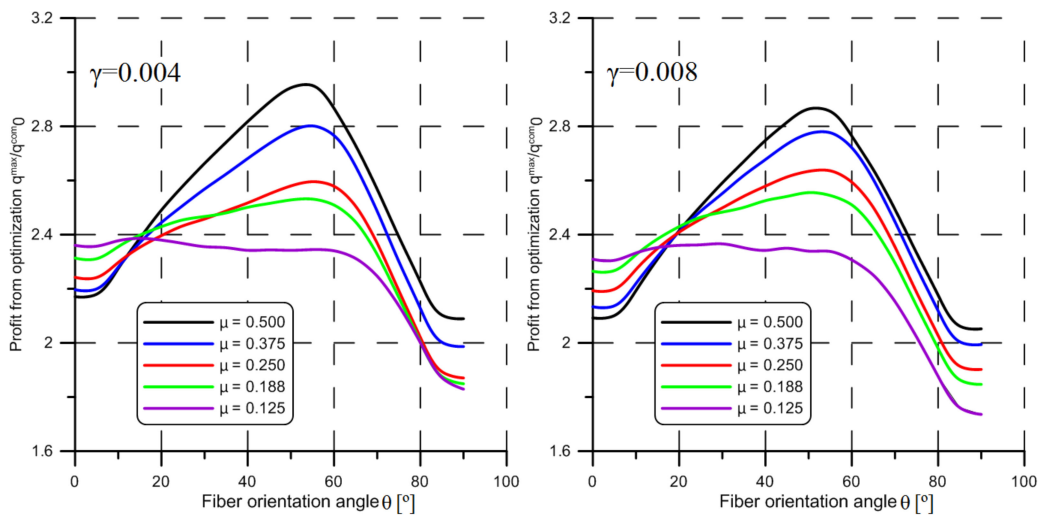


Figure 5. Optimization profit q^{max}/q^{com}_0 as a function of fiber orientation angle θ , $E_1/E_2 = 17.573$.

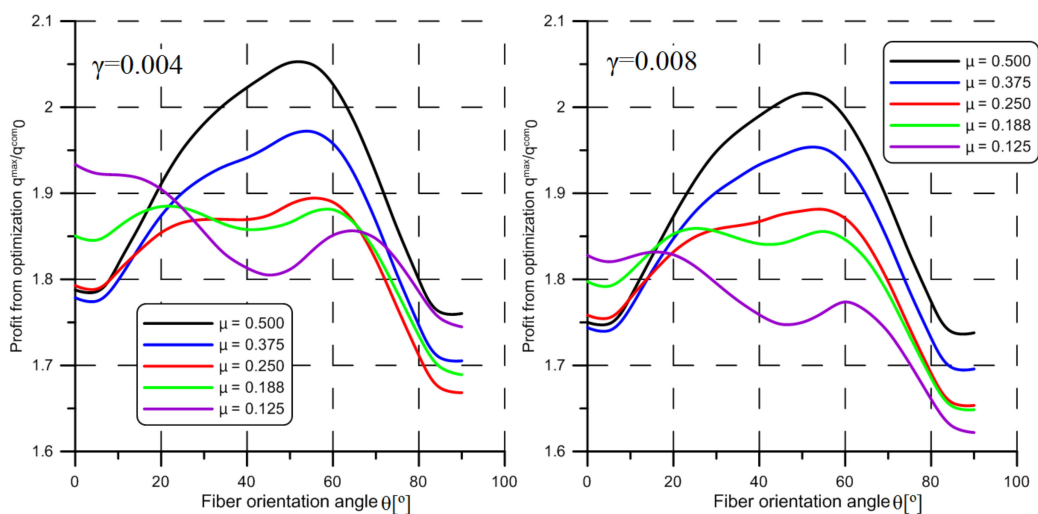


Figure 6. Optimization profit q^{max}/q^{com}_0 as a function of fiber orientation angle θ , $E_1/E_2 = 3.415$.

Table 6. Results of optimization for shell under twisting.

μ	$q_0 \cdot 10^{-6}$	q^{max}/q_0	q^{ustb}/q_0	h	n/n_0	$r(0)$	$r(1)$
$\gamma = 0.004$							
0.500	7.823	1.688	1.611	0.957	34/20	1.093	0.803
0.375	7.368	1.671	1.587	0.965	32/18	1.113	0.753
0.250	6.749	1.672	1.575	0.973	26/16	1.170	0.619
0.188	6.329	1.702	1.569	0.987	22/14	1.216	0.500
0.125	5.770	1.712	1.474	1.007	18/12	1.216	0.500
$\gamma = 0.008$							
0.500	33.552	1.638	1.502	0.957	24/16	1.093	0.803
0.375	31.668	1.619	1.487	0.959	22/14	1.126	0.728
0.250	29.129	1.623	1.468	0.970	18/12	1.182	0.590
0.188	27.334	1.651	1.453	0.987	16/12	1.216	0.500
0.125	24.928	1.651	1.365	1.007	14/10	1.216	0.500

Table 7. Results of optimization for composite shell under twisting, $E_1/E_2 = 17.573$.

μ	γ	Cylindrical Pipe			Optimal (Barrel) Shape		
		$q^{com}_0 \cdot 10^{-6}$	q^{com}_{cyl}/q^{com}_0	$\theta^{cyl} [^\circ]^1$	q^{max}/q^{com}_0	$\theta^{max} [^\circ]^1$	n/n_0
0.500	0.004	2.535	1.695	20	2.951	55	38/24
0.375		2.428	1.666	15	2.802	55	36/22
0.250		2.297	1.617	0	2.596	55	30/20
0.188		2.209	1.589	0	2.531	55	24/18
0.125		2.086	1.549	0	2.386	15	14/16
0.500	0.008	10.083	1.715	25	2.864	50	28/18
0.375		10.245	1.695	20	2.777	55	26/18
0.250		9.627	1.651	15	2.636	55	22/16
0.188		9.262	1.612	10	2.555	50	16/14
0.125		8.775	1.581	0	2.366	30	10/12

¹ layer orientations are defined as $[-\theta, +\theta, -\theta, +\theta]_s$.

Table 8. Results of optimization for composite shell under twisting, $E_1/E_2 = 3.415$.

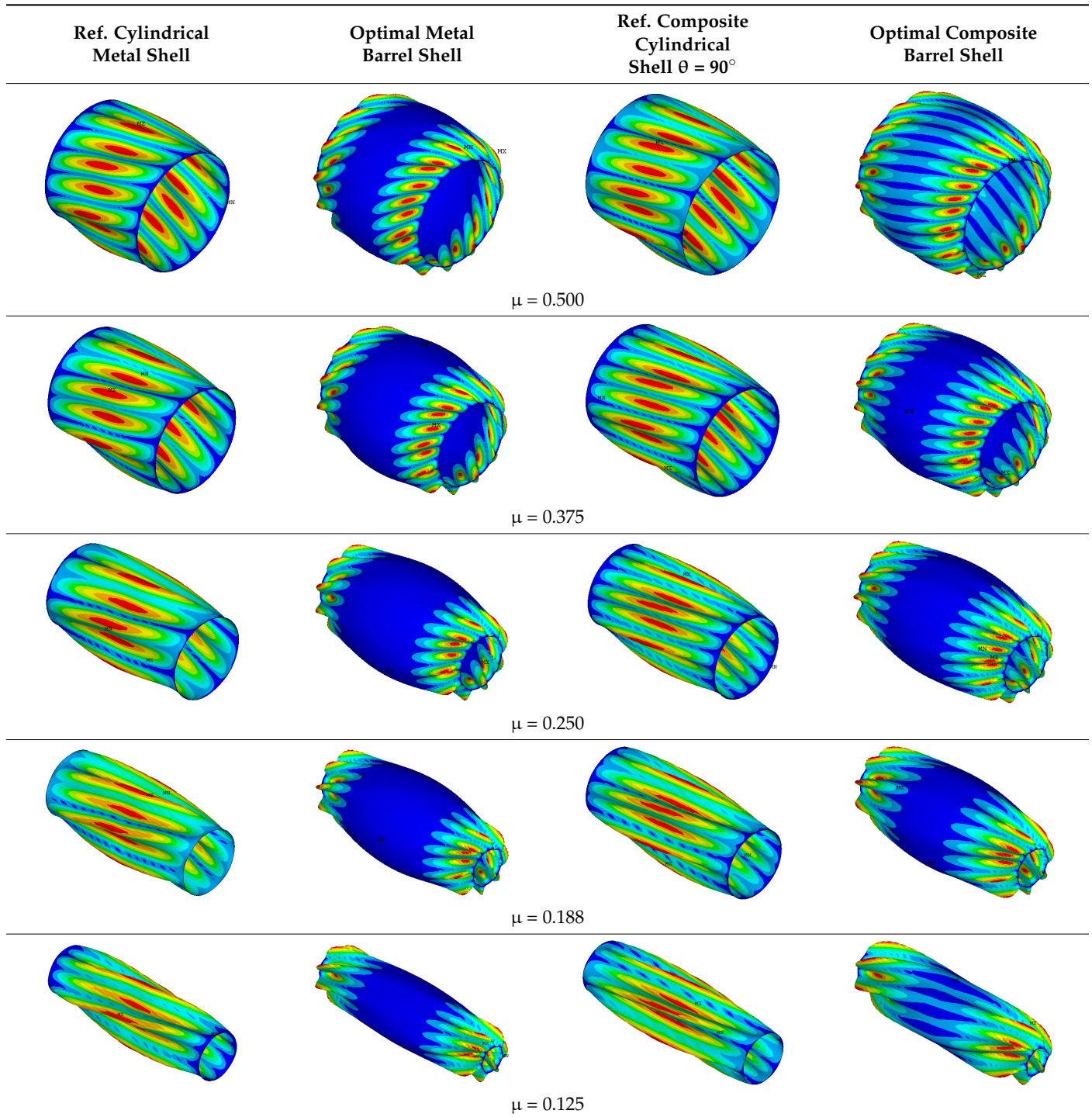
μ	γ	Cylindrical Pipe			Optimal (Barrel) Shape		
		$q^{com}_0 \cdot 10^{-6}$	q^{com}_{cyl}/q^{com}_0	$\theta^{cyl} [^\circ]^1$	q^{max}/q^{com}_0	$\theta^{max} [^\circ]^1$	n/n_0
0.500	0.004	4.552	1.238	0	2.052	50	36/22
0.375		4.362	1.233	0	1.972	55	34/20
0.250		4.100	1.221	0	1.894	55	28/18
0.188		3.911	1.214	0	1.885	20	20/16
0.125		3.602	1.214	0	1.933	0	16/14
0.500	0.008	19.259	1.244	20	2.016	50	26/16
0.375		18.368	1.240	0	1.952	50	24/16
0.250		17.280	1.232	0	1.881	55	20/14
0.188		16.562	1.219	0	1.859	25	16/12
0.125		15.539	1.207	0	1.832	15	12/12

¹ layer orientations are defined as $[-\theta, +\theta, -\theta, +\theta]_s$.

The number of half-waves is much higher in the case of optimal structures in comparison with reference ones and the number of half-waves decreases together with the decreasing value of parameter μ . Similarly, as in the case of shells under external pressure, the number of half-waves observed for the optimal structure decreases together with an increasing value of γ . On the contrary of the structure under external pressure, all half-waves are localized at both ends of the shell, what is depicted in Table 9. The center of the structure seems to be unaffected by the buckling phenomenon. Finally, starting

from $\mu = 0.188$, the inequality constraint (3), where $r(1) \geq 0.5$, is active for both values of parameter γ .

Table 9. Buckling patterns of reference and optimal shells under twisting, $\gamma = 0.008$.



As before, in the case of the second step of the optimization procedure, where the optimal fiber orientation angle is looked for, it occurred that the lowest value of the critical load multiplier is obtained for cylindrical reference where the fiber orientation angle $\theta = 90^\circ$ in all analyzed cases.

To the contrary of shells under hydrostatic pressure, in the case of shells under twisting the profit from optimization is the highest for the structures where the $\mu = 0.5$

for all investigated cases. Generally, a clear maximum can be observed in Figures 5 and 6, which correspond to the fiber orientation angle $\theta^{\max} = 50^\circ$ or $\theta^{\max} = 55^\circ$. For the shells, where $\mu = 0.188, 125$ the value of θ^{\max} is changing. The profit from optimization depends mainly on the ratio E_1/E_2 . If the E_1/E_2 ratio is greater, the observed results are also higher. The impact of parameter γ on the results are not significant as in the case of shells subjected to hydrostatic pressure. In comparison with the cylindrical shells (Tables 7 and 8), the profit from optimization is significantly higher.

Therefore, similarly to the case of shells under hydrostatic pressure, the change of the shape of the middle surface has a significant impact on the final results from optimization. Moreover, the obtained maximal values of $q^{\max}/q^{\text{com}}_0$ are higher in comparison with results, which are presented in the case of corresponding isotropic structures. Finally, as mentioned in the previous section, the buckling patterns of the optimal structures, which are made of composite material with optimal fiber orientation angle θ^{\max} , are very similar to those which are presented in Table 9. However, the number of half-waves varies significantly.

4.3. Shell under Combined Loadings

In the case of the shell structures subjected to combined loadings the main aim of carried out computations is to determine the impact of the gradually increasing twisting (the value of parameter m_t) on the solution of the optimization problem. Taking into consideration the discrepancy between the analytical and numerical results observed for the shells of uniform stability (Appendix B) under pure twisting, the appropriate comparisons are not presented now. The calculations are made for isotropic metal shells and composite shells with mechanical properties described by the ratio $E_1/E_2 = 17.573$. The results obtained for the isotropic shells for parameter $\gamma = 0.004$ and $\gamma = 0.008$ and for different values of ratio μ are summarized in Figure 7. As can be observed (Figure 7), for the isotropic shells for which the ratio $\mu = 0.5$, even a small contribution of twisting in combined loadings causes a visible reduction of the profit from optimization. In the case of the other investigated shells of uniform thickness, the obtained results are similar, which are depicted in Figure 7.

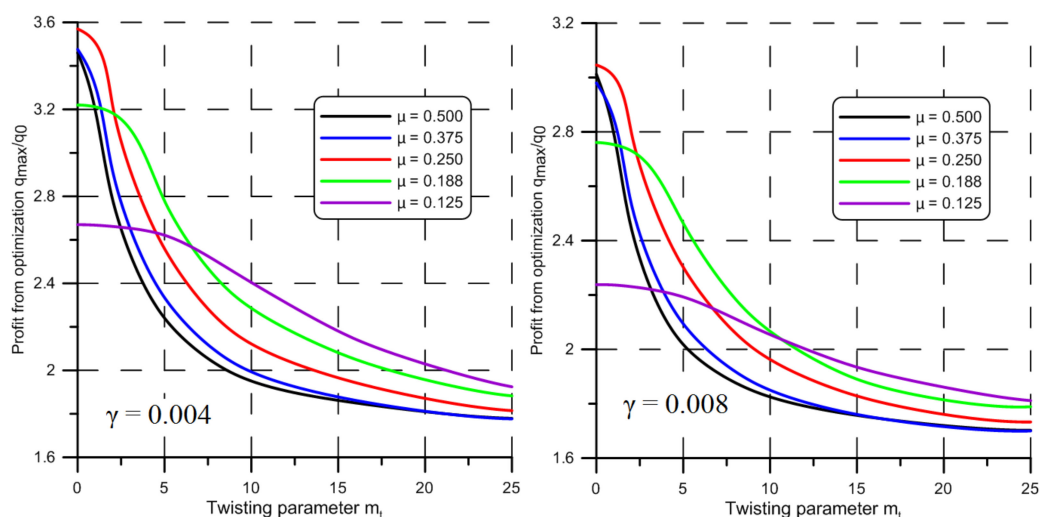


Figure 7. The profit from optimization q^{\max}/q_0 as a function of twisting parameter m_t for metal optimal barrel.

In the case of composite shells, the optimization is performed for two geometries defined by the parameters γ and μ . In the first case, in which the shell has shortened length, the parameters are equal to $\gamma = 0.004$ and $\mu = 0.5$. For such geometry, there have been two optimal geometries of the barrel-shaped shell found (see Table 2 for pure hydrostatic pressure, and Table 6 for pure twisting). In the second case, in which the shell has a shape of a long pipe, the parameters are equal to $\gamma = 0.008$ and $\mu = 0.125$. In this case, only one

shape of the optimal shape is studied. As mentioned above, $m_t = 0$ means that the studied shell is subjected to external pressure only. On the other hand, if the parameter $m_t \rightarrow \infty$, the profit from optimization, measured as q^{max}/q_0 , is expected to be identical, as in the case of pure twisting.

As can be observed in Tables 10 and 11, the obtained results strictly depend on the magnitude of the applied twisting. In both cases of the set of geometrical parameters (γ and μ) together with the increasing value of m_t (higher m_t means greater influence of twisting) the value of the critical load for the reference structures also decreases. The profit from optimization in all analyzed structures also decreases. In the case of cylindrical shells, the profit obtained from optimization is almost identical and for the relatively small values of twisting the profit is over $q^{com}_{cyl}/q^{com}_0 = 2$ and together with increasing the twisting is below $q^{com}_{cyl}/q^{com}_0 = 1.5$ for $\mu = 0.125$. However, a significantly different tendency is observed in the case of the optimal value of the fiber orientation angle θ . For the relatively small magnitude of twisting, the optimal fiber orientation angles are identical for studied cylindrical shells $\theta^{cyl} = 10^\circ$ but for the more participation of the twisting, the tendency is different. In the case of shorter structures, the value of θ^{cyl} increases to 15° and in the case of the longer ones the θ^{cyl} decreases to 0° .

Table 10. Results of optimization for composite shell under combined loadings, $\gamma = 0.004$ and $\mu = 0.5$ and $E_1/E_2 = 17.573$.

m_t	Cylindrical Pipe			Optimal (Barrel) Shape: $r^C = r(\xi = 0) = 1.115$, $r(\xi = 1) = 0.753, m = 0.325$		Optimal (Barrel) Shape: $r^C = r(\xi = 0) = 1.093$, $r(\xi = 1) = 0.803, m = 0.265$	
	$q^{com}_0 \cdot 10^{-6}$	q^{com}_{cyl}/q^{com}_0	$\theta^{cyl} [^\circ]$	q^{max}/q^{com}_0	$\theta^{max} [^\circ]^1$	q^{max}/q^{com}_0	$\theta^{max} [^\circ]^1$
0	0.781	2.090	10	5.495	15	5.359	10
0.5	0.780	2.088	10	5.221	20	5.109	15
1	0.778	2.085	10	4.988	55	4.865	60
2	0.770	2.069	5	4.616	55	4.542	60
5	0.722	1.960	10	3.872	55	3.853	55
9	0.646	1.892	15	3.476	55	3.485	55
15	0.555	1.820	15	3.249	55	3.274	55
25	0.460	1.764	15	3.101	55	3.135	55
∞ -Pure twisting	2.535	1.695	20	2.916	50	2.951	55

¹ layer orientations is defined as $[-\theta, +\theta, -\theta, +\theta]_s$.

The change of the shape of the middle surface of the structure causes a further increase in the profit from optimization. It is worth noting that in the case of the shorter shells the obtained values of the ratio q^{max}/q^{com}_0 are significantly larger in comparison with the longer ones. It should be stressed here that the optimal fiber orientation significantly differs for the structures where $\mu = 0.5$ and $\mu = 0.125$. In the first case, generally, the optimal fiber orientation angle is greater in comparison with those which are obtained in the latter case. For the shorter shells, the optimal value of θ^{max} is about 55° whereas for the longer ones the value of θ^{max} is almost constant and equal to 0° .

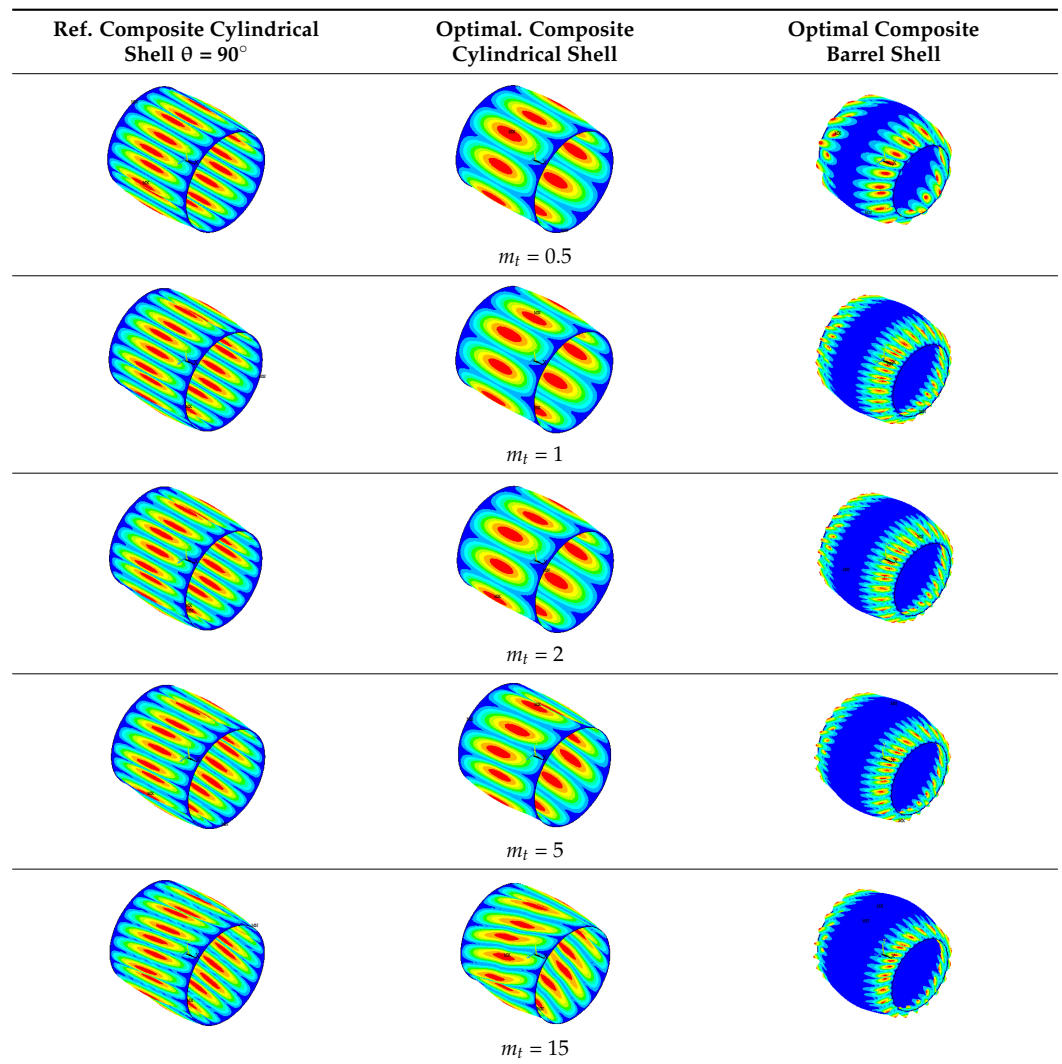
Finally, the shapes of the buckling patterns of the studied structures are presented in Table 12. Generally, it can be observed that in the case of cylindrical structures the buckling patterns obtained for all structures are very similar. The number of half-waves in the case of optimal cylindrical reference shells is generally greater in comparison with the optimal ones. However, in the case of shells of barrel shape, the buckling half-waves are generally localized in the neighborhood of the end caps of the structure. Therefore, the introduction of the variable thickness together with the change of the shape of the middle surface seems to be quite justified.

Table 11. Results of optimization for composite shell under combined loadings, $\gamma = 0.008$ and $\mu = 0.125, E_1/E_2 = 17.573$.

m_t	Cylindrical Pipe			Optimal (Barrel) Shape: $r^C = r(\xi = 0) = 1.216,$ $r(\xi = 1) = 0.500, m = 0.589$	
	$q^{com}_0 \cdot 10^{-6}$	q^{com}_{cyl}/q^{com}_0	$\theta^{cyl} [^\circ]^1$	q^{max}/q^{com}_0	$\theta^{max} [^\circ]^1$
0	1.938	2.189	10	3.386	0
0.5	1.937	2.189	10	3.385	0
1	1.936	2.186	10	3.383	0
2	1.929	2.180	5	3.372	0
5	1.891	2.100	0	3.302	0
9	1.808	1.956	0	3.146	0
15	1.669	1.825	0	2.913	0
25	1.466	1.724	0	2.678	15
∞ -Pure twisting	8.775	1.581	0	2.366	30

¹ layer orientations are defined as $[-\theta, +\theta, -\theta, +\theta]_s$.

Table 12. Buckling patterns of reference and optimal shells under twisting, $\gamma = 0.004$.



5. Conclusions

The presented work is devoted to the parametric optimization of axially-symmetric shells subjected to different loading conditions including pure external hydrostatic pressure, pure twisting, and a combination of external hydrostatic pressure and twisting. The proposed optimization procedure consists of two steps. In the first step, the optimal shape of the middle surface, as well as the constant uniform wall thickness, is looked for. In the next step, for the previously determined optimal shape of the middle surface, the optimal fiber orientation angle θ is determined. The obtained results can be summarized as follows:

1. The proposed optimization technique, based on splitting the procedure into two steps (the shape of the middle surface and the layer configuration are optimized separately), gives considerable benefits in the case of anisotropic structures subjected to combined loadings, and allows for the determination of more optimal geometries for all investigated loading conditions.
2. In the case of the isotropic structure under hydrostatic pressure, profit from optimization is the highest for structure, where $\mu = 0.5$ and $\gamma = 0.004$. The obtained q^{max}/q^0 ratio varies from 3.461 to 2.238.
3. In the case of isotropic shells subjected to pure twisting the profit from optimization varies insignificantly (from 1.712 to 1.619) and is smaller in comparison with shells under hydrostatic pressure. A very slight impact of parameters μ and γ on final results is observed.
4. Generally, in the case of composite shells, the profit from optimization is significantly higher as in the case of isotropic shells. For shells under hydrostatic pressure, the q^{max}/q^{com0} ratio varies from 5.495 to 3.386 for $E_1/E_2 = 17.573$, and from 4.080 to 2.727 for ratio $E_1/E_2 = 3.415$. The value of parameters μ and γ as well as the E_1/E_2 ratio have a significant influence on the final results.
5. For the composite shells subjected to twisting the impact of the parameters μ and γ are not significant except the E_1/E_2 ratio. The obtained results vary from 2.951 to 2.366 for $E_1/E_2 = 17.573$, and from 2.052 to 1.832 for $E_1/E_2 = 3.415$. A clear maximum in the relationship between q^{max}/q^{com0} ratio and the fiber orientation angle θ is observed.
6. In the case of structures subjected to combined load (external pressure and twisting), a significant profit of the application of the barrel-shaped shell is observed. A larger increase of this profit (q^{max}/q^{com0} is from 5.359 to 2.951) is observed for shorter shells ($\gamma = 0.004$ and $\mu = 0.5$). In the case of the longer shells, this profit is much smaller (from 3.386 to 2.366). Optimal fiber orientation angle θ^{max} is significantly different in such cases.
7. In the case of the structures, where the participation of twisting is significant, it seems to be a justified extension of the optimization procedure by the introduction of the variable thickness as the additional design variable.

Author Contributions: Conceptualization, M.B.; methodology, M.B.; software, M.B.; data curation, M.B., and P.J.R.; writing—original draft preparation, M.B., and M.C.; writing—review and editing, P.J.R., and A.S. All authors have read and agreed to the published version of the manuscript.

Funding: This research received no external funding.

Institutional Review Board Statement: Not applicable.

Informed Consent Statement: Not applicable.

Data Availability Statement: Not applicable.

Conflicts of Interest: The authors declare no conflict of interest.

Appendix A

Below, concerning the discussed previously the formulation of the optimization problem, equality and inequality constraints (Section 2), all necessary relationships are shown.

In the case of the equality constraint (1), the relationship describing the volume of material of the optimal structure and reference shell can be written as follows:

$$V_m = 4 \pi H \int_0^{\frac{L_0}{2}} R_2 dx = 2 \pi R_0 H_0 L_0. \tag{A1}$$

Next, the capacity of the optimal container is identical to the capacity of the reference structure constraint (2), namely:

$$2 \pi \int_0^{\frac{L_0}{2}} R^2 dx = 2 \pi L_0 R_0^2. \tag{A2}$$

For further computations, the following dimensionless quantities are introduced:

$$\begin{aligned} \mu &= \frac{R_0}{L_0}, \quad \gamma = \frac{H_0}{R_0}, \quad \zeta = \frac{2 \cdot x}{L_0}, \quad r = \frac{R}{R_0}, \quad r_1 = \frac{R_1}{R_0}, \quad r_2 = \frac{R_2}{R_0}, \quad h = \frac{H}{H_0}, \\ v_m &= \frac{V_m}{2 \pi L_0 R_0 H_0}, \quad q_{cr} = \sqrt{\frac{p_{cr} \sqrt{3(1-\nu_1^2)}}{2E_1}} \cdot \gamma, \quad m_t = \frac{M_t}{\pi p_0 R_0^3}, \end{aligned} \tag{A3}$$

where E_1 and ν_{12} are the material properties shown in Table 1. Then, the equality constraints (A1) and (A2) in the dimensionless form can be rewritten as follows:

$$v_m = h \int_0^1 r_2 d\zeta = 1, \quad \int_0^1 r^2 d\zeta = 1 \tag{A4}$$

Similarly, as above, the inequality constraints can be expressed in the dimensionless form as:

$$r(1) \geq r_{adm}, \quad r'' \leq 0, \quad |r'| \leq 0, \tag{A5}$$

where $(\cdot) = d/d\zeta$, $r_{adm} = R_{adm}/R_0$, $r'_{adm} = \mu R'_{adm}$. It is worth noting that the last constraint from (A5) is not taken into account in the current study.

In the dimensionless form the Equation (4), which describes the shape of the middle surface, takes the following form:

$$r(\zeta) = r^c \left(1 - m \zeta^2 \right) \tag{A6}$$

The parameter r^c denotes the radius of the middle surface measured in the middle of the shell $r^c = r(0)$. Its value can be determined with the use of equality constraint (A2). Substituting (A6) into the dimensionless form of (A2), the second relationship in (A4), the value of r^c can be written as follows:

$$r_0 = \frac{1}{\sqrt{1 - \frac{2}{3}m + \frac{1}{5}m^2}} \tag{A7}$$

Having completely defined the shape of the middle surface of the shell, the uniform constant thickness can be calculated with the use of equality constraint (A4):

$$h = \frac{1}{\int_0^1 r_2 d\zeta} \tag{A8}$$

Additionally, it is assumed that the minimum radius, the first inequality constraint in (A5), at the ends of the structure is restricted to $r(1) = r_{min} \geq 0.5$. Finally, it should be noted

here that for the shape of the middle surface, described by the expression (4), the rest of the inequality constraints in (A5) are also satisfied.

Appendix B. Local Stability Condition and Shell of Uniform Stability

The instability of thin-walled structures very often have a local character and the buckling does not depend essentially on the applied boundary condition. This is particularly true in the case of the ‘non-uniform’ geometry of a shell and the non-uniform state of stresses. In other words, instability can be determined by the stress state and the shape of a shell. The buckling phenomenon is initiated in the weakest zone of a structure. Here it is worth noting that if the thickness of the wall is relatively small in comparison with other dimensions, like the total length or diameter of a shell, the loss of stability can be more important in structural design than strength conditions. Some general theorems referring to the stability of elastic structures subjected to combined loadings are given by Papkovich [52]. One of them shows that for conservative loadings, the interaction surface is a convex one. Such a surface may also be constructed in the stress space:

$$F\left(\frac{\sigma_i}{\sigma_i^{cr}}\right) = 0 \tag{A9}$$

where σ_i^{cr} denotes critical stress. For the non-uniform stress distribution, the stresses in Equation (A9) may be considered maximal ones or stresses at certain points. Equation (A9) is called the local formulation of the stability condition. The optimization of shells with respect to their stability presents considerable difficulties connected with very complex stability equations, especially when both the middle surface and variable thickness are unknown, particularly in the case of non-uniform stress distribution. To avoid these difficulties a simplified local formulation of the stability condition should be introduced.

Making use of the hypothesis of the locality of buckling to the problem of optimal design, Życzkowski and Kruźelecki [31] proposed a concept of the shell of uniform stability which can be stated as follows: if a condition of local stability is satisfied in the form of equality not only at a dangerous point but at any point of a shell, such a structure is called ‘the shell of uniform stability’.

However, in the case of a shell with a double curvature and non-uniform (lateral and longitudinal), stress distribution application of the stability condition in the form of the Equation (A9) is practically impossible because the critical stress σ_i^{cr} for an arbitrarily shaped shell (even for single stress) is usually unknown. In those cases, Equation (A9) should be replaced by more general ones allowing for analysis of an arbitrarily shaped shell. For a shell with a double curvature, Shirshov [48] transforms the problem of global stability to a simpler problem of the local stability of such a structure. Using the linear theory of shell stability, applying the equation given by Vlassov, and assuming a sinusoidal deflection mode over a small restricted area, Shirshov obtains a rather simple formula for the critical loading parameter q , namely:

$$q = 2\sqrt{DEH} \frac{K_1 \cos^2 \phi + K_2 \sin^2 \phi}{\bar{N}_2 \cos^2 \phi + 2\bar{S} \cos \phi \sin \phi + \bar{N}_1 \sin^2 \phi}, \tag{A10}$$

where K_1 and K_2 denote meridional and circumferential curvatures, respectively. D stands for the shell stiffness, E is Young’s modulus and H is the wall thickness of the shell. The parameter ϕ is a certain variable with respect to which the critical loading multiplier q should be minimized. In Equation (A10) the membrane resultant stresses depend on q in the following way:

$$N_1 = q\bar{N}_1, N_2 = q\bar{N}_2, S = q\bar{S}, \tag{A11}$$

where S is resultant stress due to twisting. Minimization of q with respect to ϕ leads to two solutions:

$$q_{1,2} = 2\sqrt{DEH} \frac{K_1 z_{1,2}^2 + K_2}{N_2 z_{1,2}^2 + 2\bar{S}z_{1,2} + \bar{N}_1}, \tag{A12}$$

where

$$z_{1,2} = -\frac{K_1 \bar{N}_1 - K_2 \bar{N}_2}{K_1 \bar{S}} \mp \sqrt{\left(\frac{K_1 \bar{N}_1 - K_2 \bar{N}_2}{K_1 \bar{S}}\right)^2 + 4\frac{K_2}{K_1}} \tag{A13}$$

The value of critical load multiplier q is determined by one of Equation (A12), whichever leads to a smaller value. The experimental results which confirm the hypothesis of the local stability condition in the case of the shell under different loading conditions are discussed in Ref. [49]. Here it is worth noting that using different governing stability equations, Axelrad [53] also obtained the formulae (A10) describing the critical membrane resultant stresses. In the case when the resultant stress $S \equiv 0$ the critical load multiplier q is described by simpler formulae, namely:

$$q_1 = 2\sqrt{DEH} \frac{K_2}{N_1}, \quad q_2 = 2\sqrt{DEH} \frac{K_1}{N_2}, \quad q = \min(q_1, q_2) \tag{A14}$$

On the other hand, when $N_1 \equiv 0$ and $N_2 \equiv 0$ the critical load multiplier can be written as follows:

$$q = 2\sqrt{DEH} \frac{\sqrt{K_1 K_2}}{\bar{S}} \tag{A15}$$

In the case of axially-symmetric shell subjected to hydrostatic pressure and twisting the meridional resultant stress take the following form (Girkmann [54], Flügge [55]):

$$N_1 = p_0 \frac{R_2}{2R^2} (R^2 - R_{01}^2) \tag{A16}$$

where R_{01} means a radius of openings at the ends of a shell ($R_{01} = 0$ denotes closed ends of a shell). Next, taking into account the Laplace's relation between the membrane meridional and circumferential resultants, namely:

$$N_2 = p_0 R_2 - \frac{R_2}{R_1} N_1 \tag{A17}$$

the hoop resultant takes the following form:

$$N_2 = p_0 R_2 - p_0 \frac{R_2^2}{2R_1 R^2} (R^2 - R_{01}^2) \tag{A18}$$

Finally, the last resultant caused by twisting is:

$$S = \frac{M_t}{2\pi R^2} \tag{A19}$$

where M_t is a twisting moment described by Equation (1). Substituting Equations (A16) and (A18), and (A19) into (A12), the function, which describes the variable wall-thickness H , can be obtained in the most general form. This function, given in the dimensionless form is presented below (Trzeciak [56]), namely:

$$h(\xi) = q_{cr} \frac{r_2}{r} \sqrt{kr^2 \mp \sqrt{(r_{01}^2 + (k-1)r^2)^2 + \frac{k m_t^2}{r_2^2}}}, \tag{A20}$$

where

$$r_1 = -\frac{(1 + 4\mu^2 r'^2)^{\frac{3}{2}}}{4\mu^2 r''}, r_2 = r\sqrt{1 + 4\mu^2 r'^2}, k = \frac{r_1}{r_2}, r_{01} = \frac{R_{01}}{R}. \tag{A21}$$

The sign ‘±’ means that among two possible values of h the appropriate is that which provides greater wall thickness. In the case of a shell subjected to hydrostatic pressure, the function describing the wall thickness h can be computed with the use of Equation (A20) with assumption $m_t = 0$ or with the use of Equation (A14). The appropriate relationships take the following forms:

$$\begin{aligned} h(\xi) &= q_{cr} \frac{r_2}{r} \sqrt{r^2(2k - 1) + r_{01}^2}, N_2 = N_{cr}, \\ h(\xi) &= q_{cr} \frac{r_2}{r} \sqrt{r^2 - r_{01}^2}, N_1 = N_{cr}. \end{aligned} \tag{A22}$$

Finally, in the case of pure twisting, the wall thickness is described in the expression which can be obtained with the use of (1), (A15) and (A19):

$$h(\xi) = q_{cr} \frac{(r_1 r_2)^{\frac{1}{4}}}{r} \tag{A23}$$

For the shell of uniform stability, the equation describing the dimensionless volume of material v_m takes the following form:

$$v_m = \int_0^1 h(\xi) r_2 d\xi = 1 \tag{A24}$$

To verify discussed above analytical model of the shell of uniform stability, the advanced numerical procedure is proposed. This procedure is based on the finite element method and it consists of the following steps:

1. First of all, the maximal value of critical load multiplied and the corresponding shape of the middle surface of the shell is determined with the use of Equations (A6), (A7), and (A24). The variable wall thickness is described by one of the expressions (A20), (A22), or (A23) depending on which case of the load is studied.
2. The determined previously optimal shape of the middle surface is imported to the system of the finite element method. Next, the regular mesh, which consists of quadrilateral elements, is generated as shown in Figure 2. The size of the elements is assumed as $l_e = L_0/40$.
3. It is assumed that the thickness in each finite element is constant and its value is computed with the use of the expression (A20), (A22), or (A23) in the point where $\xi = (\xi_i + \xi_{i+1})/2, i = 1, 2, \dots, 40$. Of course, the mentioned coordinates ξ_i and ξ_{i+1} describe the X coordinate of the nodes which create each following ring of finite elements. For all these elements the wall thickness H is identical.
4. For such a finite element model the buckling analysis is performed. If the value of the obtained critical load multiplier is identical in comparison with the value computed with the use of analytical formulas described in Appendix B, which means that the analytical model provides reliable and accurate results.

The verification is performed for the isotropic shells subjected to pure external hydrostatic pressure and pure twisting. The obtained results are presented in Tables A1 and A2. As can be observed in the case of pure external pressure the numerical and analytical results are relatively similar. It is worth noting that generally the loss of stability is caused by the circumferential resultant stress N_2 . However, in the case of the shell where $\mu = 0.5$, there are the zones where the buckling is caused by the meridional resultant stress N_1 . The presented in Table A1 results are obtained for such structures where only circumferential resultant stress N_2 causes the loss of stability in the whole shell. In other words, the critical load

multiplier computed with the use of the case where $N_2 = N_{cr}$ always gives smaller values of q_{cr} in comparison with the case where $N_1 = N_{cr}$. Generally, the discrepancy does not exceed 2% in all investigated cases. However, in the case of pure twisting, a significant discrepancy is observed. This can be caused by the fact that the assumed approximation of the resultant stress S , Equation (A19), is very rough. Therefore, the comparison of the optimal solutions is presented only in the case of isotropic structures subjected to external pressure.

Table A1. Optimal shell of uniform stability under hydrostatic pressure.

μ	$q_0 \cdot 10^{-6}$	q^{ustb}/q_0	q^{mes}/q_0	n/n_0	$r(0)$	$r(1)$
$\gamma = 0.004$						
0.500	2.500	3.953	3.961	70/16	1.137	0.702
0.375	2.162	3.934	3.945	74/14	1.216	0.500
0.250	1.773	3.547	3.573	42/10	1.216	0.500
0.188	1.517	3.233	3.263	30/10	1.216	0.500
0.125	1.223	2.750	2.791	20/8	1.216	0.500
$\gamma = 0.008$						
0.500	11.811	3.347	3.356	50/12	1.137	0.702
0.375	10.364	3.282	3.293	52/12	1.216	0.500
0.250	8.457	2.975	3.007	30/10	1.216	0.500
0.188	7.115	2.757	2.798	12/8	1.216	0.500
0.125	5.903	2.279	2.325	14/6	1.216	0.500

Table A2. Optimal shell of uniform stability under twisting.

μ	$q_0 \cdot 10^{-6}$	q^{ustb}/q_0	q^{mes}/q_0	n/n_0	$r(0)$	$r(1)$
$\gamma = 0.004$						
0.500	7.823	1.611	1.813	44/20	1.093	0.803
0.375	7.368	1.587	1.839	42/18	1.115	0.753
0.250	6.749	1.575	2.015	40/16	1.170	0.619
0.188	6.329	1.569	2.237	38/14	1.216	0.500
0.125	5.770	1.474	2.123	28/12	1.216	0.500
$\gamma = 0.008$						
0.500	33.552	1.502	1.669	30/16	1.093	0.803
0.375	31.668	1.487	1.762	30/14	1.126	0.728
0.250	29.129	1.468	1.928	30/12	1.181	0.590
0.188	27.334	1.453	2.081	28/12	1.216	0.500
0.125	24.928	1.365	1.978	20/10	1.216	0.500

References

1. Pan, B.B.; Cui, W.C. An overview of buckling and ultimate strength of spherical pressure hull under external pressure. *Mat. Struct.* **2010**, *23*, 227–240. [CrossRef]
2. Zingoni, A. Liquid-containment shells of revolution: A review of recent studies on strength, stability and dynamics. *Thin Wall. Struct.* **2015**, *87*, 102–114. [CrossRef]
3. Blachut, J.; Magnucki, K. Strength, Stability, and optimization of pressure vessels: Review of selected problems. *Appl. Mech. Rev.* **2008**, *61*, 60801. [CrossRef]
4. Liu, P.; Kaewunruen, S.; Zhou, D.; Wang, S. Investigation of the Dynamic Buckling of Spherical Shell Structures Due to Subsea Collisions. *Appl. Sci.* **2018**, *8*, 1148. [CrossRef]
5. Blachut, J. Buckling of cylinders with imperfect length. *J. Press. Technol.* **2014**, *137*, 011203. [CrossRef]
6. Xue, J. Local buckling in infinitely, long cylindrical shells subjected uniform external pressure. *Thin Wall. Struct.* **2012**, *53*, 211–216. [CrossRef]
7. MacKay, J.R.; Van Keulen, F.; Smith, M.J. the accuracy of numerical collapse predictions for the design of submarine pressure hulls. *Thin Wall. Struct.* **2011**, *49*, 145–156. [CrossRef]
8. Blachut, J. Buckling of externally pressurized steel toriconical shells. *Int. J. Press.Vessel. Pip.* **2016**, *144*, 25–34. [CrossRef]

9. Zhang, J.; Zhang, M.; Tang, W.X.; Wang, W.B.; Wang, M.L. Buckling of spherical shells subjected to external pressure: A comparison of experimental and theoretical data. *Thin Wall. Struct.* **2017**, *111*, 58–64. [[CrossRef](#)]
10. Błachut, J. Experimental perspective on the buckling of pressure vessel components. *Appl. Mech. Rev.* **2013**, *66*, 11003. [[CrossRef](#)]
11. Sato, M.; Wadee, M.A.; Iiboshi, K.; Sekizawa, T.; Shima, H. Buckling patterns of complete spherical shells filled with an elastic medium under external pressure. *Int. J. Mech. Sci.* **2012**, *59*, 22–30. [[CrossRef](#)]
12. Shakouri, M.; Kouchakzadeh, M.A. Analytical solution for vibration of generally laminated conical and cylindrical shells. *Int. J. Mech. Sci.* **2017**, *131–132*, 414–425. [[CrossRef](#)]
13. Krysko, V.A.; Awrejcewicz, J.; Saveleva, N.E. Stability, bifurcation and chaos of closed flexible cylindrical shells. *Int. J. Mech. Sci.* **2008**, *50*, 247–274. [[CrossRef](#)]
14. Thompson, J.; Michael, T. Advances in shell buckling: Theory and experiments. *Int. J. Bifurc. Chaos* **2015**, *25*, 1530001. [[CrossRef](#)]
15. Arbocz, J.; Starnes, J.H. Future directions and challenges in shell stability analysis. *Thin Wall. Struct.* **2002**, *40*, 729–754. [[CrossRef](#)]
16. Błachut, J. On optimal barrel - shaped shells under buckling constraints. *AIAA J.* **1987**, *25*, 186–188.
17. Błachut, J. Combined axial and pressure buckling of shells having optimal positive curvature. *Comput. Struct.* **1987**, *26*, 513–519. [[CrossRef](#)]
18. Błachut, J. Buckling of externally pressurised barrelled shells: A comparison of experiment and theory. *Int. J. Pres. Ves. Pip.* **2002**, *79*, 507–517. [[CrossRef](#)]
19. Błachut, J. Optimal barreling of steel shells via simulated annealing algorithm. *Comp. Struct.* **2003**, *81*, 1941–1956. [[CrossRef](#)]
20. Jasion, P.; Magnucki, K. Elastic buckling of barrelled shell under external pressure. *Thin Wall. Struct.* **2007**, *45*, 393–399. [[CrossRef](#)]
21. Jasion, P. Stability analysis of shells of revolution under pressure conditions. *Thin Wall. Struct.* **2009**, *47*, 311–317. [[CrossRef](#)]
22. Jasion, P.; Magnucki, K. Elastic buckling of horizontal barrelled shells filled with liquid—Numerical analysis. *Thin Wall. Struct.* **2012**, *52*, 117–125. [[CrossRef](#)]
23. Magnucki, K.; Jasion, P. Analytical description of pre-buckling and buckling states of barrelled shells under radial pressure. *Ocean Eng.* **2013**, *58*, 217–223. [[CrossRef](#)]
24. Krużelecki, J.; Stawiarski, A. Optimal design of thin-walled columns for buckling under loadings controlled by displacements. *Struct. Multidiscip. Optim.* **2010**, *42*, 305–314. [[CrossRef](#)]
25. Zhang, J.; Wang, M.; Wang, W.; Tang, W. Buckling of egg-shaped shells subjected to external pressure. *Thin Wall. Struct.* **2017**, *113*, 122–128. [[CrossRef](#)]
26. Zhang, J.; Hua, Z.; Tang, W.; Wang, F.; Wang, S. Buckling of externally pressurised egg-shaped shells with variable and constant wall thickness. *Thin Wall. Struct.* **2018**, *132*, 111–119. [[CrossRef](#)]
27. Zhang, J.; Tan, J.; Tang, W.; Zhao, X.; Zhu, Y. Experimental and numerical collapse properties of externally pressurized egg-shaped shells under local geometrical imperfections. *Int. J. Pres. Ves. Pip.* **2019**. [[CrossRef](#)]
28. Sowiński, K. Buckling of shells with special shapes with corrugated middle surfaces—FEM study. *Eng. Struct.* **2019**, *179*, 310–320. [[CrossRef](#)]
29. Rezaiee-Pajand, M.; Masoodi, A.R. Shell instability analysis by using mixed interpolation. *J. Braz. Soc. Mech. Sci. Eng.* **2019**, *41*, 419. [[CrossRef](#)]
30. Rezaiee-Pajand, M.; Arabi, E.; Masoodi, A.R. Nonlinear analysis of FG-sandwich plates and shells. *Aerosp. Sci. Technol.* **2019**, *87*, 178–189. [[CrossRef](#)]
31. Życzkowski, M.; Krużelecki, J. Optimal design of shells with respect to their stability. In *IUTAM Symposium on Optimization in Structural Design*; Sawczuk, A., Mróz, Z., Eds.; Springer: Warsaw, Poland, 1973; Berlin/Heidelberg, Germany; New York, NY, USA, 1975; pp. 229–247.
32. Krużelecki, J.; Trzeciak, P. Optimal design of axially symmetrical shells under hydrostatic pressure with respect to their stability. *Struct. Multidisc. Optim.* **2000**, *19*, 148–154. [[CrossRef](#)]
33. Życzkowski, M.; Krużelecki, J.; Trzeciak, P. Optimal design of rotationally symmetric shells for buckling under thermal loadings. *J. Appl. Mech.* **2001**, *39*, 443–455.
34. Barski, M.; Krużelecki, J. Influence of a shearing force on optimal design of shells against buckling under overall bending. *Eng. Optim.* **2004**, *36*, 439–455. [[CrossRef](#)]
35. Barski, M.; Krużelecki, J. Optimal design of shells against buckling by means of the simulated annealing method. *Struct. Multidisc. Optim.* **2005**, *29*, 61–72. [[CrossRef](#)]
36. Barski, M.; Krużelecki, J. Optimal design of shells against buckling under overall bending and external pressure. *Thin Wall. Struct.* **2005**, *43*, 1677–1698. [[CrossRef](#)]
37. Barski, M. Optimal design of shells against buckling subjected to combined loadings. *Struct. Multidisc. Optim.* **2006**, *31*, 211–222. [[CrossRef](#)]
38. Muc, A.; Chwał, M.; Barski, M. Remarks on experimental and theoretical investigations of buckling loads for laminated plated and shell structures. *Compos. Struct.* **2018**, *203*, 861–874. [[CrossRef](#)]
39. Barski, M.; Romanowicz, P. Natural frequencies and modal shapes of composite cylindrical panels with local damages. In *Shell Structures: Theory and Applications—Proceedings of the 10th SSTA 2013 Conference*; Gdańsk, Poland, 16–18 October 2013; Pietraszkiewicz, W., Górski, J., Eds.; Taylor & Francis Group: London, UK, 2014; Volume 3, pp. 277–280.

40. Muc, A.; Bondyra, A.; Romanowicz, P. Buckling of composite multilayered shells—An experimental analysis. In *Shell Structures: Theory and Applications—Proceedings of the 10th SSTA 2013 Conference*; Gdańsk, Poland, 16–18 October 2013, Pietraszkiewicz, W., Górski, J., Eds.; Taylor & Francis Group: London, UK, 2014; Volume 3, pp. 227–230.
41. Muc, A.; Stawiarski, A.; Romanowicz, P. Experimental Investigations of Compressed Sandwich Composite/Honeycomb Cylindrical Shells. *Appl. Compos. Mater.* **2018**, *25*, 177–189. [[CrossRef](#)]
42. Stawiarski, A.; Chwał, M.; Barski, M.; Muc, A. The influence of the manufacturing constraints on the optimal design of laminated conical shells. *Compos. Struct.* **2020**, *235*, 111820. [[CrossRef](#)]
43. Muc, A.; Chwał, M.; Romanowicz, P.; Stawiarski, A. Fatigue-Damage Evolution of Notched Composite Multilayered Structures under Tensile Loads. *J. Compos. Sci.* **2018**, *2*, 27. [[CrossRef](#)]
44. Muc, A. Peculiarities in the Material Design of Buckling Resistance for Tensioned Laminated Composite Panels with Elliptical Cut-Outs. *Materials* **2018**, *11*, 1019. [[CrossRef](#)]
45. Verchery, G. Design rules for the laminate stiffness. *Mech. Compos. Mater.* **2011**, *47*, 47–58. [[CrossRef](#)]
46. Muc, A.; Chwał, M. Analytical discrete stacking sequence optimization of rectangular composite plates subjected to buckling and FPF constraints. *J. Theor. Appl. Mech.* **2016**, *54*, 423–436. [[CrossRef](#)]
47. Vlassov, V.S. *Allgemeine Schalentheorie und ihre Anwendung in der Technik*; Akademie-Verlag: Berlin, Germany, 1958; (translated from Russian, Moskva-Leningrad 1949).
48. Shirshov, V.P. Local buckling of shells. *Soviet Appl. Mech.* **1966**, *2*, 77–78. [[CrossRef](#)]
49. Bushnell, D. *Computerized Buckling of Shells. Mechanics of Elastic Stability 9*; Martinus Nijhoff Publishers: Dordrecht, The Netherlands, 1985.
50. Muc, A. *Mechanika Kompozytów Włóknistych*; Księgarnia Akademicka: Kraków, Poland, 2003.
51. Bere, P.; Nemes, O.; Dulescu, C.; Berce, P.; Sabau, E. Design and analysis of carbon/epoxy composite tubular parts. *Adv. Eng. Forum* **2013**, *8–9*, 207–214. [[CrossRef](#)]
52. Papkovich, P.F. *Stroitel'naya Mekhanika Korablya, Ch. 2. (Structural Mechanics of a Ship), Part 2*; Gos. Soyuz. Izd. Sudostr. Promyshl: Leningrad, Russia, 1941. (in Russian)
53. Axelrad, E.I. On local buckling of thin shells. *Int. J. Non Linear Mech.* **1985**, *24*, 249–259. [[CrossRef](#)]
54. Grikmann, K. *Flächentragwerke, Einführung in die Elastostatik der Scheiben, Platten, Schalen und Faltwerke*; Springer: Berlin/Heidelberg, Germany, 1954.
55. Flügge, W. *Statik und Dynamik der Schalen*; Springer: Berlin/Heidelberg, Germany, 1957.
56. Trzeciak, P. Optimal Design of Axially-Symmetric Shells of Uniform Stability Subjected to Combined Loadings. Ph.D. Thesis, Cracow University of Technology, Kraków, Poland, 2006. (in Polish).